8-2008

Dynamical behavior and influence of stochastic noise on certain generalized Boolean networks

Gary L. Beck
University of Nebraska Medical Center

Mihaela Teodora Matache
University of Nebraska at Omaha, dvelcsov@unomaha.edu

Dynamical Behavior and Influence of Stochastic Noise on Certain Generalized Boolean Networks

Gary L. Beck[1], **Mihaela T. Matache**[2*]

[1] Department of Pediatrics University of Nebraska Medical Center, Omaha, NE 68198-2184

[2]Department of Mathematics, University of Nebraska at Omaha, Omaha, NE 68182-0243
Phone: 402-554-3295, Fax: 402-554-2975, *dmatache@mail.unomaha.edu

Abstract: This study considers a simple Boolean network with N nodes, each node's state at time t being determined by a certain number of parent nodes. The network is analyzed when the connectivity k is fixed or variable. Making use of a Boolean rule that is a generalization of Rule 22 of elementary cellular automata, a generalized formula for providing the probability of finding a node in state 1 at a time t is determined. We show typical behaviors of the iterations, and we study the dynamics of the network through Lyapunov exponents, bifurcation diagrams, and fixed point analysis. We conclude that the network may exhibit stability or chaos depending on the underlying parameters. In general high connectivity is associated with a convergence to zero of the probability of finding a node in state 1 at time t. We also study analytically and numerically the dynamics of the network under a stochastic noise procedure. We show that under a smaller probability of disturbing the nodes through the noise procedure the system tends to exhibit more nodes in the same state. For many parameter combinations there is no critical value of the noise parameter below which the network remains organized and above which it behaves randomly.

PACS codes: 05.45.-a, 02.70.-c, 89.75.-k, 84.35.+i

Keywords: random Boolean network, generalized elementary cellular automata rule 22, system dynamics, chaos, stochastic noise, dynamical phase transition.

1. Introduction

A Boolean network can function as a model for a large class of real or artificial networks from the brain to ecology as shown for example by Wuensche's work [1], genetic regulatory networks with papers by Shmulevich, Dougherty et. al. ([2], [3], [4]), chemical processes with works such as the paper by Heidel et. al. [5], biology with papers such as the ones by Klemm and Bornholdt ([6], [7]), and Raeymaekers [8], neural networks in Aldana and Cluzel's paper [9], Huepe and Aldana [10], physical networks in papers by Marr and Hütt ([11], [12]), and artificial life in Wolfram's works such as [13]. Boolean network models have been used for modelling networks in which the node or cell activity can be described by two states, 1 and 0, ON and OFF, "active and nonactive", "responsive and non-responsive", "up-regulated and down-regulated", and in which each node is updated based on logical relationships with other nodes. In fact, Stuart Kauffman originally developed random Boolean networks as a model for genetic regulatory networks [14]. They have been referred to as $N-K$ models or Kauffman networks.

There are 256 elementary cellular automata (ECA) rules outlined by Wolfram [13]. We will be concerned with one rule in particular, namely Rule 22, which is a Class III rule in Wolfram's characterization. Class I rules lead to an absorbing state; Class II rules lead to periodicity; Class III rules lead to chaos; and Class IV rules lead to more complex behavior with fairly simple localized structures interacting in complicated ways. Thus Classes III and IV are of greater interest. As observed by Matache and Heidel [17], rule 22 is both "legal", reflection symmetric with $(0,0,0) \to 0$,

and "totalistic", where the rule depends only on the relative number of ON and OFF states and not their order ([15]). There are 32 legal rules, and 16 totalistic rules. The formulae used in this paper hold for Boolean networks governed by totalistic rules. Only 8 of the legal and totalistic rules, including Rule 22, are in both classes. These eight thereby distinguished rules are # 0, 22, 104, 126, 128, 150, 232, 254. They separate into Wolfram's four classes as: Class I: 0, 128, 254; Class II: 104, 232; Class III: 22, 126, 150; Class IV: none. Besides the automata in Class I and Class II which have relatively simple behavior ([13]), this leaves only three: # 22, 126, and 150. But # 150 is additive (linear in algebraic form) which simplifies its analysis by transferring unusual effects from the structure of the automata to the initial conditions only. As well as Rule 22 and Rule 126 both being in Wolfram's Class III, they are also both in the same $\kappa = 2$ in a new classification regarding separating planes for the basic 8 point hypercube (along with # 104) ([16]). As observed in [17], both Rule 126 and Rule 22 have a natural and simple interpretation in terms of the growth of cell colonies. For Rule 126, complete crowding of live, ON, cells causes death, OFF, in the next generation. Complete isolation of a potential cell prevents birth in the next generation. A similar interpretation holds for Rule 22; however, it is not quite as absolute: a cell is turned ON at the next time step if and only if exactly one node in the cell's neighborhood is ON and the others are OFF. It is of interest to explore the dynamics of networks of arbitrary sizes and neighborhoods evolving under these two rules subject to various scenarios. This implies the need for generalizations of these rules to varying neighborhood sizes.

We point out that a comprehensive work has been done on exploring random Boolean networks governed by a generalized ECA Rule 126 in papers such as the ones by one of the authors of this paper and collaborators for synchronous or asynchronous networks, with fixed or variable number of parent nodes or inputs, with or without noise ([17], [18], [19], [20], [21], [22]). However, an extension of Rule 22 has not been considered so far in similar contexts. In this study we propose a new generalized ECA Rule 22 and identify the dynamics of a network governed by variants of this generalization. The dynamic analysis parallels previous methods published in the papers mentioned above. The dynamics of the network indicate order, through multiple attractors and bifurcations, or chaos, depending on the underlying parameters. As opposed to the dynamics of Rule 126, there are no reversed bifurcations, and large connectivity drives the proportion of active nodes to zero. We show that under certain assumptions the proposed generalization can be considered a threshold function in a neural network, or a biologically meaningful function that generates a bias between the number of activators and inhibitors in a biological network that can be modelled as a Boolean net.

Properties of Boolean networks have been considered in a variety of studies. For example, the dynamical organization in the presence of noise of certain Boolean neural networks with random connections has been studied by Huepe and Aldana [10], who show that there is a critical value of a noise parameter that generates a dynamical phase transition in the network. In that case if the noise parameter surpasses the critical value, the nodes are basically activated or inactivated in a random manner, so the proportion of active nodes is driven to 0.5. On the other hand, Goodrich and Matache [20] use similar types of stochastic noise with constraints on the number of perturbed nodes for a synchronous network evolving by the generalized ECA Rule 126. In that case the noise can have a stabilizing effect on the network and the proportion of active nodes can be driven to 1. In this paper we consider the approach of [10] to investigate the reaction of the network to perturbations for the proposed generalized ECA Rule 22. We show that there may be no dynamical

phase transition, and the proportion of active nodes may decrease linearly to 0.5 with the increase of the noise parameter.

Thus, this paper presents a new in-depth study of a single generalized cellular automaton rule on Boolean networks with fixed or varying connectivity. We make use of a mean field approximation for Boolean networks governed by the class of totalistic ECA rules investigated by Andrecut [23], to describe the probability of finding a node in state 1 at time t in Section 2, and investigate the dynamics of a Boolean network under a new specific generalized ECA Rule 22 with a random parent assignment. We show the good match of the formula to the Boolean system by comparing simulated dynamics with the analytical description in Section 3. For certain parameter combinations we analyze the dynamics of the system by exploring bifurcation diagrams and Lyapunov exponents in Section 4, and fixed points in Section 5. Then in Section 6 the reaction of the network to stochastic noise is investigated. We define an order parameter and obtain both analytic and numerical results to estimate it. We show that there is no critical value of the noise parameter that differentiates between ordered and random behavior of the system. Section 7 is dedicated to conclusions and further directions of research.

2. The Boolean Network

Consider a network with N nodes. Each node c_n, $n = 1, 2, \ldots, N$ can take on only two values 0 or 1. The connectivity of the nodes is fixed throughout the evolution of the system, but the nodes are allowed to have different numbers of parent nodes. The parents of a node are chosen randomly from the remaining $N-1$ nodes and do not change thereafter. Thus if a node has k parents, then a set of k parents is chosen from the remaining $N-1$ nodes with probability $1/\binom{N-1}{k}$. At each time step t, a fraction $\alpha(t) \in [0, 1]$ of nodes is updated. The case $\alpha(t) = 1$ corresponds to a synchronous network. This will be our main focus in this study. For simplicity we assume that all the nodes in each class of nodes with a fixed number of parents k_j update according to the same rule at a given time step t, and the rule does not change with time. A similar approach is used for a generalized ECA Rule 126 in [17], [21]. Note that varying Boolean rules lead to a quenched network whose dynamics can approximate the dynamics of a corresponding annealed network in the thermodynamic limit $N \to \infty$.

A totalistic cellular automata rule depends only on the number of parents in state 1. Given a node c_n with k_j parents, a totalistic rule for that node can be expressed as a pair of Boolean functions $(r_0^{k_j}, r_1^{k_j}) : \{0, 1, 2, \ldots, k_j\}^2 \to \{0, 1\}$ such that $c_n(t+1) = r_0^{k_j}(s)$ if $c_n(t) = 0$, and $c_n(t+1) = r_1^{k_j}(s)$ if $c_n(t) = 1$, where s is the sum of the values of the parents of node c_n at time t. A general formula for the probability $p(t+1)$ of a node being in state 1 at time $t+1$, given $p(t)$ was obtained in [23]. The author uses a mean field approach to show that the dynamical evolution of the network can be described by a family of polynomial maps. The results hold in the thermodynamic limit $N \to \infty$, the only case where chaos is possible, since otherwise the networks are eventually periodic. This formula is applicable to the class of legalistic rules and in a more general setting to the class of probabilistic Boolean networks in which a node can be updated according to more than one Boolean rule to account for natural variations and disturbances in the system. Probabilistic Boolean networks have been studied by Shmulevich et. al. [2], and future work will consider an extension of the analysis in this paper to that kind of networks.

The formula for $p(t+1)$ can be expressed as follows:

$$p(t+1) = \sum_{j=1}^{J} C_j g_{k_j}(t) \tag{1}$$

where $g_{k_j}(t) = [1-\alpha(t)]p(t)+\alpha(t)\sum_{s=0}^{k_j}\gamma(p(t), r_0^{k_j}(s), r_1^{k_j}(s))P_{s,k_j}(p(t))$ and $\gamma(p(t), r_0^{k_j}(s), r_1^{k_j}(s)) = (1-p(t))r_0^{k_j}(s) + p(t)r_1^{k_j}(s)$, with $P_{s,k_j}(p(t)) = \binom{k_j}{s}p(t)^s(1-p(t))^{k_j-s}$. Here $k_j, j = 1, 2, \ldots J$ are the possible values for the number of parents, $C_j, j = 1, 2, \ldots, J$ are the fractions of nodes with k_j parents (so $\sum_{j=1}^{J} C_j = 1$), $\alpha(t)$ is the fraction of nodes to be updated at time t, and s is the number of parents of node c_n that are in state 1.

The ECA Rule 22 maps a node $c_n(t)$ to state 1 at time $t+1$ if and only if exactly one of its parents has value 1, that is if exactly one-third of its parents are in state 1. A node is its own parent in the ECA. We propose to extend this rule to a network of size N with an arbitrary number of inputs per node by using the following general rule:

$$c_n(t+1) = \begin{cases} 1 & \text{if} \quad d_1 \leq d \leq d_2 \\ 0 & \text{if} \quad \text{otherwise} \end{cases} \tag{2}$$

where d is the fraction of 1s in the neighborhood of node c_n. Thus $d = \frac{s}{k+1}$ if node $c_n(t) = 0$, or $\frac{s+1}{k+1}$ if node $c_n(t) = 1$, where s is the number of parents in state 1 at time t, and k is the connectivity of node c_n. Here $0 \leq d_1 \leq d_2 \leq 1$ are fixed parameters. The rule basically states that node c_n is turned ON if and only if the fraction of parents in state 1 is within the bounds d_1 and d_2; otherwise the node is turned OFF. We also assume that the node is turned OFF under complete isolation or complete crowding. If the network has 3 nodes and $d_1 = d_2 = \frac{1}{3}$ we obtain the ECA Rule 22. Hung et al. [24] have used a simpler generalization of ECA Rule 22 in the context of synchronization of stochastically coupled random Boolean networks: a node is turned ON if and only if a single parent is ON. The new generalization provided in (2), allows us to analyze a wider variety of totalistic rules and provides an insight into Boolean systems governed by rules meaningful for neural networks or biology. For instance, observe that if $d_2 = 1$ then the output is 1 (or it fires) if and only if the sum of all the inputs is at least the threshold $0 < d_1 < 1$. Thus in this case we deal with a Boolean linear threshold function with equal weights that is typical for neural networks. This kind of networks were the subject of "threshold logic" in the 1960's [25], and have been studied further for example by Anthony [26]. On the other hand, one could consider that a small value of d_1 implies that fewer active inputs have the property of activating the node under consideration. Thus there is a bias towards the activators of the node. If d_1 is large then there is a bias towards the inhibitors of the node. It is known that biologically meaningful Boolean functions have input elements that are activators or inhibitors, which can act alone or in conjunction with other activators and/or inhibitors, as specified by Raeymaekers [8]. That author has shown that in an ECA governed by biologically meaningful functions with 3 or 4 inputs, increasing significantly the bias towards the inhibitors or the activators has the effect of decreasing the length of the cycles and of the run-ins (the initial part of trajectories before cycles are reached). It is of interest to understand what are the dynamics in the case of a more general network, since real biological networks do not necessarily have only a few inputs, and could be non-directed, that is the number of inputs and outputs of a node need not be the same. Thus a varying number of parent nodes and a random parent assignment would provide a more general understanding of the phenomenon.

Now let us provide the approximation formula for the probability of a node being in state 1 for rule (2). The notation $[x]$ is used to indicate the integer part of x. Observe that under rule (2) we have $r_0^{k_j}(s) = 1$ for $d_1^j \leq s/(k_j+1) \leq d_2^j$, and 0 otherwise. Given that $s \in \{1, \ldots, k_j\}$, we get $r_0^{k_j}(s) = 1$ for $s \in \{1, \ldots, k_j\} \cap [d_1^j(k_j+1), d_2^j(k_j+1)]$ and 0 otherwise. Similarly one can see that $r_1^{k_j}(s) = 1$ for $s \in \{0, 1, \ldots, k_j - 1\} \cap [d_1^j(k_j+1) - 1, d_2^j(k_j+1) - 1]$ and 0 otherwise. Thus we have the following result on the approximation formula for the probability of finding a node in state 1.

Proposition: Under the assumption of a Boolean network evolving according to rule (2) and with the characteristics specified in formula (1), the probability $p(t+1)$ of a node being in state 1 at time $t+1$ given $p(t)$ can be written as $p(t+1) = [1-\alpha(t)]p(t) + \alpha(t)\sum_{j=1}^{J} C_j g_{k_j}(t)$ where

$$g_{k_j}(t) = \sum_{s \in A_0^{k_j}} \binom{k_j}{s} p(t)^s (1-p(t))^{k_j - s + 1} + \sum_{s \in A_1^{k_j}} \binom{k_j}{s} p(t)^{s+1} (1-p(t))^{k_j - s}. \tag{3}$$

Here $A_0^{k_j} = \{1, \ldots, k_j\} \cap [d_1^j(k_j+1), d_2^j(k_j+1)]$ and $A_1^{k_j} = \{0, 1, \ldots, k_j - 1\} \cap [d_1^j(k_j+1) - 1, d_2^j(k_j+1) - 1]$. The values $0 \leq d_1^j \leq d_2^j \leq 1, j = 1, 2, \ldots, J$ are the fixed fractions in rule (2) and they can vary for nodes with different number of parents. However, all the nodes with a given number of parents evolve according to the same rule.

Next we iterate formula (3) and compare the results with the frequencies of ones obtained from evolving an actual Boolean network governed by the rule described in this section, to identify how well the approximation formula matches the Boolean network evolution.

3. Iterations of the Network

Using Matlab, we generate iterations of both formula (3) and the Boolean network for many initial conditions under the same parameter choices and graph them on the same plot. We include figures with parameter combinations that yield typical results chosen from numerous simulations. For each parameter combination we perform 256 iterations of both formula (3) and the frequencies of ones obtained from the evolution of the Boolean network and we plot the results on the same graph for comparison and to identify behavioral trends. We consider the cases of fixed connectivity k and two distinct connectivity values k_1 and k_2 in the network. In each simulation we fix the parameters d_1 and d_2 as well as the fractions C_1 and C_2 when applicable. Figure 1 is representative of trends in the dynamical behavior of a network with fixed connectivity. The parameters d_1 and d_2 are chosen to indicate the various possible trends; other parameter combinations yield similar results. After one iteration there is an excellent match for all three cases. After 256 iterations, the match is good although not necessarily as good as in the case of the first iteration. We observe that for $k = 2$ the probability of finding a node in state 1 and the frequency of ones for the Boolean network reach a horizontal plateau at $p \simeq 0.45$. For $k = 4$, a more dynamic behavior is observed: there appears to be a region of $p(t)$ with two co-existing end states which are the consequence of two fixed points as we will see in the bifurcation diagrams. In general, a similar behavior is related to the existence of higher order fixed points. Finally, when $k = 16$ we observe convergence to 0. Note that the first iteration yields multiple fixed points, but only the origin is attracting, the other fixed points being repellers. These trends are observed in general for various parameter combinations. It is noted that a large connectivity is associated with convergence to zero.

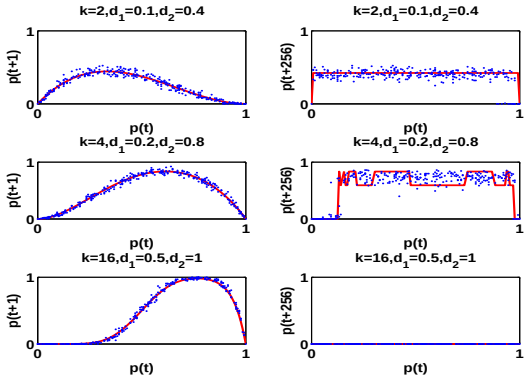

FIGURE 1. Matching behavior of the frequency of ones for the Boolean network (dots) and the probability of finding a node in state 1 given by formula (3) (continuous curve) for fixed connectivity of k randomly assigned parents. Here the network has $N = 128$ nodes. We choose many initial values of $p(t) \in [0, 1]$ and iterate the formula and evolve the Boolean network a number of times computing the new values of $p(t)$ at each time step. We show a selection of three parameter combinations as specified in the titles of the subplots, and plot $p(t+1)$ and $p(t+256)$ for comparison. We observe the almost perfect match after one iteration and a similar behavior after 256 iterations in all cases. We also note the differences in the long run behavior for the various scenarios considered. This figure is typical for the case of fixed connectivity. In the first case there appears to be an attracting fixed point, in the second case a period two orbit, while a large connectivity is associated with one attracting fixed point at the origin with basin the entire interval $[0, 1]$.

For the case of variable connectivity k, we focus on only two possible values for the number of parents, k_1 and k_2. For three or more values, the simulations become extremely time consuming due to a significant increase of parameter combinations to be considered. Therefore we focus only on two values of k. We use various values for M_1, the number of nodes with k_1 parents. Figure 2 is representative. Here we fix $N = 128, k_1 = 10, k_2 = 32$, while the values of M_1 are specified in each pair of graphs. Also, $M_2 = N - M_1$. The first two lines demonstrate stability and a good match after 256 iterations. The first case indicates the existence of an attracting fixed point, while in the second case there is a convergence to zero with the exception of $p(t) \simeq 0.65 - 0.95$ suggesting the existence of two distinct attracting fixed points. The third case is suggestive of period two orbits and finally, the last case shows convergence to 0 after 256 iterations, with the origin being the only attracting fixed point. These trends are observed in general for various parameter combinations, and the larger the network the better the matches.

4. Bifurcation Diagrams and Lyapunov Exponents

In this section we present bifurcation diagrams and corresponding Lyapunov exponent (LyE) computations to provide a further understanding of the dynamics of the system. To generate the bifurcation diagrams, we first fix all the parameters except the connectivity k which is allowed to vary. For each value of k formula (3) is iterated a number of times to pass the transient phase and then the resulting values of $p(t)$ are plotted on the vertical line passing through k for many initial conditions. In addition one needs to analyze the sensitivity of the orbits to initial values. This is done mainly through the computation of the LyE which provide an approximation for the average

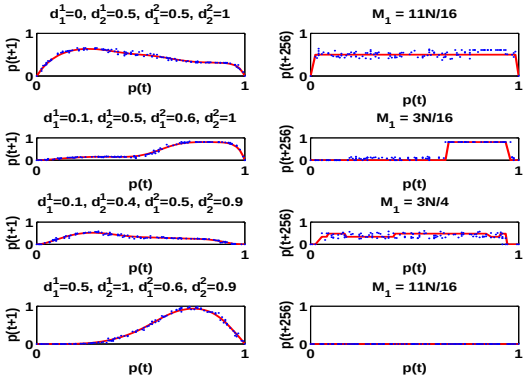

FIGURE 2. Analog of Figure 1 for variable connectivity k and randomly assigned parents. Here $N = 128, k_1 = 10$, $k_2 = 32$, and the other parameters are as specified in the titles (all the parameters indicated in the two titles of each line correspond to both graphs on each line). Again we observe the almost perfect match after one iteration and a similar behavior after 256 iterations in all cases. We also note the differences in the long run behavior for the various scenarios. This figure is typical for the case of two possible connectivity values. The first two cases indicate the existence of attracting fixed points: a single one in the first case, and two distinct ones in the second case. The third case suggests the existence of stable period two orbits, while the last case shows that the origin is the only attracting fixed point.

multiplicative rate of divergence or convergence of orbits starting at nearby points. The LyE is defined to be $L(x_0; f) = \lim_{n\to\infty} \left[\prod_{j=0}^{n-1} |f'(x_j)|\right]^{1/n}$, where $f(x)$ is the map describing the evolution of the system from one time step to another, and $\{x_0, x_1, \ldots, x_n \ldots\}$ represents the trajectory of x_0 under the map f. When the LyE of an orbit is negative, the implication is that a stable orbit is attained. Conversely, when the LyE is positive, the implication is that chaos is present, provided the orbit is not asymptotically periodic [27]. On the other hand there could exist orbits that are asymptotically periodic and with positive LyE. It should be noted that LyE are undefined for some orbits, particularly an orbit containing a point x_i with $f'(x_i) = 0$.

Observe that in the case of the formula (1), to compute the LyE we use the function

$$f(p) = (1-\alpha)p + \alpha \sum_{j=1}^{J} C_j \sum_{s=0}^{k_j} [(1-p) r_0^{k_j}(s) + p r_1^{k_j}(s)] \binom{k_j}{s} p^s (1-p)^{k_j - s}. \tag{4}$$

In the simulations we fix the number of nodes to $N = 128$, and we iterate the system 1000 time steps before plotting the bifurcation diagrams versus integer k values. In Figure 3 we present two samples for a network with fixed connectivity k. When $d_1 = 0.1$ and $d_2 = 0.4$ we can see that as the value of k increases both the LyE and the bifurcation diagram suggest chaos. A similar situation is noted for $d_1 = 0.2$ and $d_2 = 0.8$ and $k = 8$; for the other values of k the system exhibits both positive and negative values of the LyE, whereas the bifurcation diagram suggests multiple attractors. For $k < 8$ the LyE could be positive or negative since we can identify multiple attractors, so the orbits are eventually periodic.

We note that similar graphs are obtained for other parameter combinations, for fixed or variable connectivity, and are not included to make the paper concise. In general we observe that smaller values of connectivity are associated with periodic attractors with negative or positive LyE (mostly

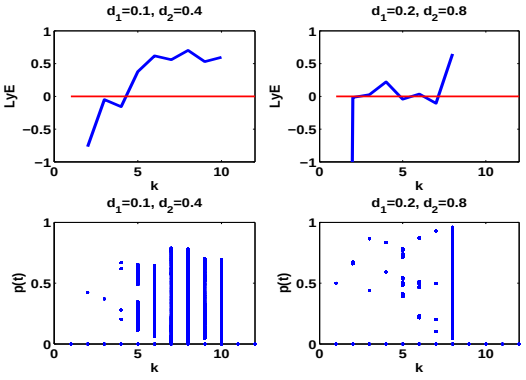

FIGURE 3. LyE and bifurcation diagrams for selected parameters with $N = 128$. When $d_1 = 0.1$ and $d_2 = 0.4$ we can see that as the value of k increases ($k > 4$), both the LyE and the bifurcation diagram suggest chaos. For $d_1 = 0.2$ and $d_2 = 0.8$ and $k = 8$ the same is observed, while for the other values of k the bifurcation diagrams are not very spread out, and the exponents take on positive or negative values. (Note: the LyE for $k = 1$ in case of $d_1 = 0.2$ and $d_2 = 0.8$ is much smaller than -1. However we have chosen the given window of values for more clarity of the plots.)

close to zero), with a passage to chaos and positive LyE as the connectivity increases. Large connectivity values induce convergence to the origin which is the only attracting fixed point, and thus the LyE are not defined.

5. Focus on Fixed Points

It is useful to understand how the fixed points of the map behave. To do this we need to solve the equation $f(p) = p$ where $f(p)$ is given in formula (4). Observe that this equation can be written as $p = \sum_{j=1}^{J} C_j \sum_{s=0}^{k_j} [(1-p) r_0^{k_j}(s) + p r_1^{k_j}(s)] \binom{k_j}{s} p^s (1-p)^{k_j - s}$. Now $p = 0$ is automatically a fixed point since $r_0^{k_j}(0) = 0$. We will start this section by analyzing this case in more detail. Later we will focus on the special case of the generalized Rule 22.

Observe that $f'(0) = (1-\alpha) + \alpha \sum_{j=1}^{J} C_j \{[-r_0^{k_j}(0) + r_1^{k_j}(0)] - k_j r_0^{k_j}(0) + k_j r_0^{k_j}(1)\} = \sum_{j=1}^{J} C_j [r_1^{k_j}(0) + k_j r_0^{k_j}(1)]$ since $r_0^{k_j}(0) = 0$ and $\alpha = 1$. For simplicity we will discuss in detail the stability of the origin in the case when the values $r_0^{k_j}$ and $r_1^{k_j}$ are either 0 or 1 for all $k_j > 1$.

Case 1: $r_1^{k_j}(0) = r_0^{k_j}(1) = 0$ for all k_j. Observe that $|f'(0)| = 0$ so the origin is stable. If the values of k_j are large enough and the values of the corresponding d_1^j in the generalization of Rule 22 are also large enough, then this case is satisfied automatically. This is in agreement with the previous observations that in many cases the probability $p(t)$ converges to 0.

Case 2: $r_1^{k_j}(0) = 0$ and $r_0^{k_j}(1) = 1$ for all k_j. Then $|f'(0)| = \sum_{j=1}^{J} C_j k_j$. Observe that $\sum_{j=1}^{J} C_j k_j = C_1(k_1 - k_J) + C_2(k_2 - k_J) + \cdots + C_{J-1}(k_{J-1} - k_J) + k_J$. We can always order the connectivity values such that $k_1 > k_2 > \cdots > k_J$. Thus all the terms $k_j - k_J$ are nonnegative in the expression above and thus the entire expression is at least $k_J > 1$. Therefore the origin is unstable for any value of J.

Case 3: $r_1^{k_j}(0) = 1$ and $r_0^{k_j}(1) = 0$ for all k_j. Then $f'(0) = \sum_{j=1}^{J} C_j = 1$ so we cannot make decisions about the stability of 0.

Case 4: $r_1^{k_j}(0) = r_0^{k_j}(1) = 1$ for all k_j. Then $f'(0) = \sum_{j=1}^{J} C_j(1+k_j) = 1 + \sum_{j=1}^{J} C_j k_j > 1$ which means that the origin is unstable.

In conclusion, for the special case when the Boolean rules are chosen such that the values $r_1^{k_j}(0)$ and $r_0^{k_j}(1)$ are the same for all connectivity values k_j, the origin could be stable or unstable per the cases above, and there are situations in which we cannot make a decision based on the value of $f'(0)$.

Let us focus on the generalized Rule 22 now for the case of a synchronous network with fixed connectivity, so $J = 1$. We can rewrite formula (3) as $p(t+1) = \sum_{s\in A_0^k} \binom{k}{s} p(t)^s (1-p(t))^{k-s+1} + \sum_{s\in A_1^k} \binom{k}{s} p(t)^{s+1}(1-p(t))^{k-s}$ where $A_0^k = \{1,\ldots,k\} \cap [d_1(k+1), d_2(k+1)]$ and $A_1^k = \{0,1,\ldots,k-1\} \cap [d_1(k+1)-1, d_2(k+1)-1]$. Thus, we will study the fixed points of the following function

$$f(p) = \sum_{s\in A_0^k} \binom{k}{s} p^s (1-p)^{k-s+1} + \sum_{s\in A_1^k} \binom{k}{s} p^{s+1}(1-p)^{k-s} \tag{5}$$

Note that we have used the same notation $f(p)$ although this is a new function. The discussion that follows refers to the function (5). We start by solving the equation $f(p) = p$ numerically for various combinations of the parameters k, d_1, d_2. However we will present in detail the two cases studied in the previous section, namely $d_1 = 0.1, d_2 = 0.4$ and $d_1 = 0.2, d_2 = 0.8$. Using Matlab we compute the fixed points for these two scenarios for $k \leq 20$ and we plot them in Figure 4. We also compute the values of $f'(p)$ for the fixed points obtained and we plot them on the right hand side of Figure 4 as specified in the subplots. We observe that the origin is not the only fixed point. The values of $f'(p)$ are plotted as follows: $f'(0)$ is marked by a star, the values $f'(p)$ for fixed points with values less than 0.3 are marked with an x, while the remaining fixed points are marked with a +. We also plot the lines $f'(p) = -1$ and $f'(p) = 1$. Observe that the origin is stable for most values of k. Only for $k = 1$ or 2 there may be a stable fixed point other than the origin. However, in light of the previous bifurcation diagrams, we know that the basin of attraction of the origin cannot be the entire interval $[0, 1]$.

Let us discuss the case $d_1 = 0.2, d_2 = 0.8$ in detail. If $k = 1$ we obtain $f(p) = 2p(1-p)$ which is a logistic equation with $p = 0$ unstable fixed point and $p = 1/2$ stable fixed point, with basin $(0, 1)$. If $k = 2$, $f(p) = 3p(1-p)$ for which the origin is unstable but $p = 2/3$ is a stable fixed point with basin $(0, 1)$. Note that $f'(2/3) = -1$ which corresponds to a point where a period-doubling bifurcation occurs. If $k = 3$ the function becomes a polynomial of degree 4 with only two roots in $[0, 1]$, namely 0 and 0.7221. Both are unstable, but the equation $f^2(p) = p$ yields a stable period-2 orbit $\{0.4410, 0.8645\}$ which corresponds to the bifurcation diagram in Figure 3. Iterations of the function $f(p)$ indicate no other higher order periodic orbits, so the period-2 orbit has basin $(0, 1)$. However, if $k = 4$ observe that $p = 0$ is a stable fixed point. We obtain also two other fixed points, $p = 0.1312$ and $p = 0.7487$ which are both unstable. The basin of the origin is $[0, 0.1312)$. We obtain also a period-2 stable orbit, $\{0.5929, 0.8341\}$. Higher order iterates do not show any higher order periodic orbits. This is similar to the bifurcation diagram for $k = 4$ and corresponds to the observations made for Figure 1 (second set of graphs). In Figure 5 we graph the function (5) and iterations $f^2(p), f^4(p)$ and $f^8(p)$ for $k = 4, 5, 8$. For $k = 4$ we observe that the higher order iterates do not generate further intersections with the main diagonal. For $k = 5$ we observe that the origin is a stable fixed point, but the period-2 orbit $\{0.4384, 0.76\}$ is unstable. However, period-4 orbits occur as well. This corresponds to the observations in the bifurcation diagram. We include also

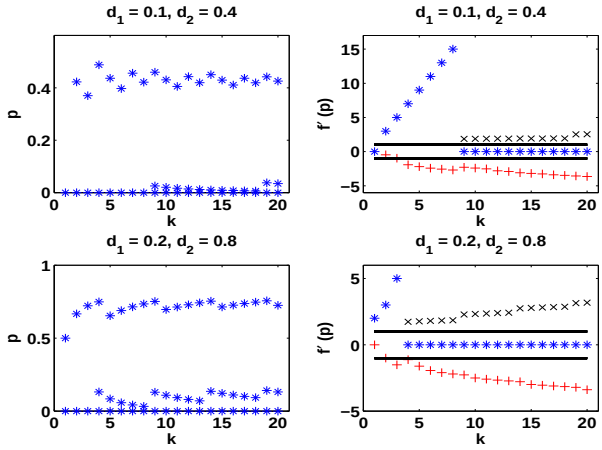

FIGURE 4. Fixed points of the function (5), $f(p) = \sum_{s\in A_0^k} \binom{k}{s} p^s(1-p)^{k-s+1} + \sum_{s\in A_1^k} \binom{k}{s} p^{s+1}(1-p)^{k-s}$ in the first column for the specified values of d_1 and d_2 and the corresponding values of $f'(p)$ in the second column. Here the origin is marked by a star, the fixed points with values less than 0.3 are marked with an x, while the remaining fixed points are marked with a +. We observe the existence of multiple fixed points for all the values of k. The origin is stable in most cases, although its basin of attraction may not be the entire interval $[0, 1]$.

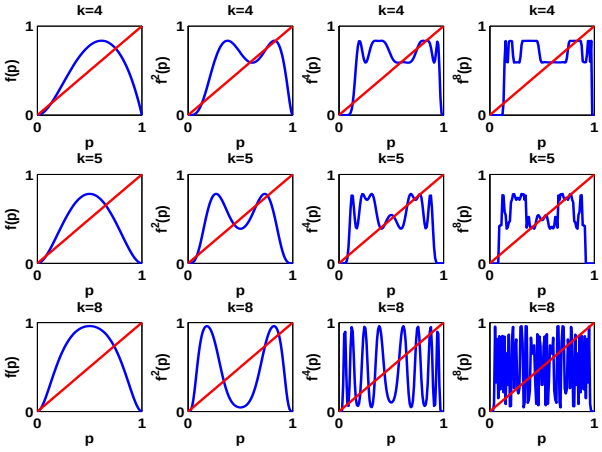

FIGURE 5. Plots of $f(p), f^2(p), f^4(p)$ and $f^8(p)$ for the function (5), $f(p) = \sum_{s\in A_0^k} \binom{k}{s} p^s(1-p)^{k-s+1} + \sum_{s\in A_1^k} \binom{k}{s} p^{s+1}(1-p)^{k-s}$. We consider the cases $k = 4, 5$, and 8 by lines, for $d_1 = 0.2, d_2 = 0.8$. We observe more complexity for $k = 5$ and the existence of numerous higher order periodic orbits for $k = 8$.

the case $k = 8$ to emphasize the existence of numerous higher order periodic orbits. At the same time, for $k > 8$ we observe that the iterations converge to zero.

Similar observations are made for other parameter combinations. As a matter of fact one could see that the condition for the stability of the fixed point 0 can be obtained by figuring out if one 1 in a network of 0s will lead to more than one 1 in the network in the next time step. So if a node is in state 0 and only one of its k parents in state 1, the origin is unstable if $\frac{1}{k+1} \in [d_1, d_2]$.

For instance if $d_1 = 0.2, d_2 = 0.8$, then the origin is unstable for $k = 1, 2, 3$ and stable for $k \geq 4$ since in that case $\frac{1}{k+1} < 0.2$. Similarly, if $d_1 = 0.1, d_2 = 0.4$, the origin is stable for $k = 1$ since $\frac{1}{k+1} = 0.5 > d_2$, unstable for $k = 2, 3, \ldots, 9$, and stable again for $k > 9$. These observations match the results discussed above.

6. Dynamics under Stochastic Noise

Now let us analyze the dynamical behavior of the system under stochastic noise. We discuss in detail the case of fixed connectivity k. To this aim we define a random procedure for changing the state of each node at each time step. The rule introduces a noise intensity parameter η. Note that the Boolean rule (2) is given by the following function $g(c_{n_1}, c_{n_2}, \ldots, c_{n_{k+1}}) = \chi_{[d_1(k+1), d_2(k+1)]}\left(\sum_{j=1}^{k+1} c_{n_j}\right)$, where χ represents the characteristic function of the interval $[d_1(k+1), d_2(k+1)]$, meaning that the function is null everywhere except when $\sum_{j=1}^{k+1} c_{n_j} \in [d_1(k+1), d_2(k+1)]$, and in that case the function is equal to 1. The nodes $\{c_{n_1}, c_{n_2}, \ldots, c_{n_{k+1}}\}$ represent the k parents of node c_n together with the node itself. At each time step t we introduce the following stochastic noise procedure:

$$c_n(t+1) = \begin{cases} g(c_{n_1}, c_{n_2}, \ldots, c_{n_{k+1}}) & \text{with probability} \quad 1-\eta \\ 1 - g(c_{n_1}, c_{n_2}, \ldots, c_{n_{k+1}}) & \text{with probability} \quad \eta \end{cases} \tag{6}$$

where $\eta \in [0, 1/2]$. If $\eta = 0$ the dynamics are purely deterministic and given by the analysis in previous sections, while for $\eta = 1/2$ they are purely random. This type of noise has been previously considered by Huepe and Aldana-González [10] in the case of a neural network model with noise. The authors consider a neural network evolving according to a Boolean function given by the sign of a weighted linear combination of the inputs. They show that the system exhibits a phase transition at a critical noise intensity parameter η_c which is computed analytically and numerically. In what follows we propose an approach similar to [10] and we show that a phase transition may not occur in the context of the Boolean rules used in this paper. Basically noise means driving the proportion of 1s in the network to 0.5. If the attracting fixed point without noise has a much larger (or smaller) proportion of 1s, a phase transition may occur. For example, in the previous sections we saw that a larger k yields an attracting fixed point at the origin, so the nodes become 0 eventually, which means that the proportion of 0s converges to 100%. However, if noise is applied, as the noise parameter η increases the proportion of 0s and 1's will approach 0.5 and intuitively there could be a clear dynamical phase transition. On the other hand, if the network is attracted towards a higher order cycle or behaves chaotically, then the other parameters of the system would become essential in determining the reaction of the system to the noise.

As in [10] we define the order parameter

$$\Psi = \lim_{T\to\infty} \frac{1}{T - T_0} \int_{T_0}^{T} |s(t)|\, dt \qquad \text{where} \qquad s(t) = \lim_{N\to\infty} \frac{1}{N} \sum_{n=1}^{N} (2c_n(t) - 1). \tag{7}$$

Here T_0 is arbitrarily chosen. Observe that for a system in which most elements are in the same state we have $|s(t)| \approx 1$, whereas for a system in which the elements randomly take values 0 or 1 we have that $|s(t)| \approx 0$. Our goal is to provide a mathematical relation between η and Ψ and compare it with numerical results obtained for the real system.

First we consider the quantity $\phi(t) \equiv P_t(\{c_n = 1\}) = \lim_{N\to\infty}(1/N)\sum_{n=1}^{N} c_n(t)$, where the last equality represents the thermodynamic limit of the fraction of nodes in state 1 at time t, which thus becomes the probability of finding any node in state 1 at time t. Then $\phi(t) = (s(t)+1)/2$. Now let $\xi(t) = \sum_{j=1}^{k+1} c_{n_j}(t)$, which can be considered a sum of independent random variables. Using the notation $P_{\xi(t)}(x)$ for the probability distribution function associated to ξ and $P_{c(t)}(x)$ for the probability distribution function associated to c_{n_j} we get $P_{\xi(t)}(x) = P_{c(t)} * P_{c(t)} * \cdots * P_{c(t)}(x)$, where $*$ denotes the convolution of the $k+1$ identical functions. Then the probability that $g = 1$ at time t is $I(t) \equiv P_t(\{g = 1\}) = \sum_x P_{\xi(t)}(x)$, where $x \in [d_1(k+1), d_2(k+1)] \cap \mathbf{N}$. Then clearly $\phi(t+1) = I(t)(1-\eta) + (1-I(t))\eta$. It follows that $s(t+1) = (2\eta-1)(1-2I(t))$.

Note that $P_{c(t)}(1) = \phi(t)$ and $P_{c(t)}(0) = 1-\phi(t)$ and thus we deal with a Bernoulli random variable with parameter $\phi(t)$. Then $\xi(t)$ becomes a binomial distribution with parameters $k+1$ and $\phi(t)$. This implies that $I(t) = \sum_x \binom{k+1}{x}\phi(t)^x(1-\phi(t))^{k+1-x} = (1/2^{k+1})\sum_x \binom{k+1}{x}(1+s(t))^x(1-s(t))^{k+1-x}$, where $x \in [d_1(k+1), d_2(k+1)] \cap \mathbf{N}$. We are interested in the fixed points of the function given by $s(t+1) = (2\eta-1)(1-2I(t))$ with $I(t)$ expressed in terms of $s(t)$ as above, since the quantity $s(t)$ will approach the fixed points as $t \to \infty$. Thus we need to solve

$$s = (2\eta-1)\left[1 - \frac{1}{2^k}\sum_x \binom{k+1}{x}(1+s)^x(1-s)^{k+1-x}\right] \tag{8}$$

for various values of η. We do this numerically, and we obtain $\Psi = |s|$ from the analytic expression (8) as a function of η. We plot the results and compare them with the numerical computations of the integral (7) obtained directly from a system with $N = 512$ nodes that has been evolved a few hundred time steps under the noise rule (6) for various values of the noise parameter η. Observe that if $\eta \to 1/2$ then the right hand side of (8) approaches zero, so $s \to 0$. Thus, we expect to see a convergence to zero of the values of Ψ as η increases from 0 to 1/2.

In Figure 6 we show typical results for only a couple of values of d_1 as specified in the plots and $d_2 = 1$. As mentioned previously in this case we deal with a Boolean linear threshold function that is typical for neural networks. Recall also that small values of d_1 imply that fewer active inputs have the property of activating the node under consideration. Thus there is a bias towards the activators of the nodes. If d_1 is large then there is a bias towards the inhibitors of the nodes. In Figure 6 we compute numerically the values of Ψ from formula (8) for different noise levels η and plot the resulting values with dots. For the same values of the noise parameter we also compute the values of Ψ obtained from formula (7) and plot them with stars. We observe the very good match, and that as $\eta \to 1/2$ we have that $\Psi \to 0$. The larger the network the better the match. On the other hand we note that for $d_1 = 0.45$ there is a clear phase transition that occurs around $\eta = 0.3$, while for $d_1 = 0.75$ no such transition occurs. This is observed in general for various values of k: medium values of d_1 may generate a phase transition while other values of d_1 correspond to a rather linear decrease to zero. We will show analytically that this is indeed the case for certain parameter combinations, but that in many cases there is no phase transition. We can see that for small values of η, meaning a smaller probability of disturbing the nodes through the noise procedure, the system tends to exhibit more nodes in the same state since Ψ is close to 1. However, for large values of the noise parameter η the nodes tend to take on randomly the values 1 and 0.

We also plot the first and the fourth iteration of the function (8) in Figure 7. This is done for $d_1 = 0.25, 0.45, 0.55, 0.75$ and for $\eta = 0.1, 0.2, 0.3, 0.4$. We graph the first iteration with interrupted line and the fourth iteration is with continuous line. Observe that as η increases the intersection

with the first diagonal gets closer to zero. On the other hand, for small η the intersection is close to 1 or -1. Also note that there is a symmetry in the function behavior as d_1 crosses 0.5. This is due to the reversed roles of the values 0 and 1 in the network as there is a bias towards the inhibitors. For example, the behavior for $d_1 = 0.45$ is similar to that for $d_1 = 0.55$ reversed by symmetry. At the same time, for medium values of d_1 we see that there can be more than one fixed point. But in general, higher order iterations do not become more complex, and no higher order fixed points are generated.

Now, let us analyze the case of even k. We have that $\sum_{x=0}^{k/2} \binom{k+1}{x} = \sum_{x=k/2+1}^{k+1} \binom{k+1}{x} = 2^k$. Therefore $s = 0$ is a solution of equation (8), so the origin is a fixed point. If $d_1 > 0$ this happens for values of d_1 and d_2 such that $[d_1(k+1), d_2(k+1)] \cap \mathbf{N} = \{k/2+1, \ldots, k+1\}$. It is immediate to see that if $d_2 = 1$ and $\frac{k}{2(k+1)} < d_1 \leq \frac{k+2}{2(k+1)}$ this is automatically satisfied. However this interval centered at $1/2$ becomes narrower as k increases. In this case for small enough values of η there are other fixed points as well, while for large values of η the origin is the only fixed point. Thus there is a critical value η_c such that for $\eta > \eta_c$ we have $\Psi = 0$. For instance, it is not hard to see by a straightforward computation of the fixed points from equation (8) that if $k = 2$ and $1/3 < d_1 \leq 2/3$, then for values $\eta > \eta_c = 1/6$ the origin is the only fixed point. Similarly, if $k = 4$ and $2/5 < d_1 \leq 3/5$, we have $\eta_c = 7/30$. The value of η_c increases with k, thus the phase transition occurs for larger η as the connectivity increases.

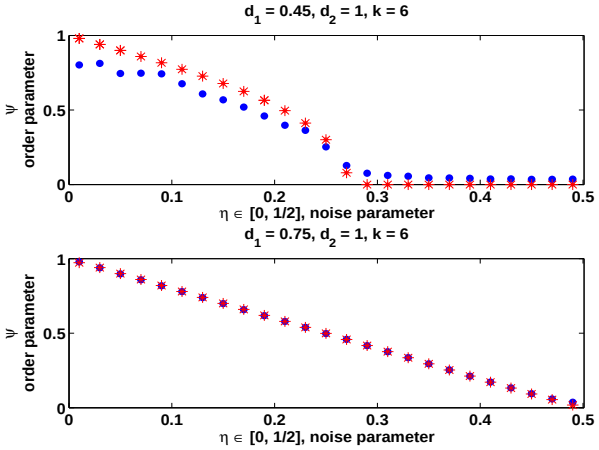

FIGURE 6. Plots of values of the order parameter Ψ versus the level of the noise parameter η for two typical values of d_1 as specified in the titles and $k = 6$. The stars represent the results of the analytic computation obtained from formula (8), namely $\Psi = |s|$, where $s = (2\eta - 1)\left[1 - \frac{1}{2^k}\sum_x \binom{k+1}{x}(1+s)^x(1-s)^{k+1-x}\right]$. The dots represent the values obtained numerically from the definition (7) of Ψ, namely $\Psi = \lim_{T\to\infty} \frac{1}{T-T_0}\int_{T_0}^{T} |s(t)|\, dt$, where $s(t) = \lim_{N\to\infty} \frac{1}{N}\sum_{n=1}^{N}(2c_n(t) - 1)$, obtained from iterations of the real system under the noise procedure. We observe that Ψ decreases with increased η and that for smaller η the values are close to 1, meaning that most nodes are in the same state. As $\eta \to 1/2$ the values of Ψ indicate a phase transition at $\eta = 0.3$ for $d_1 = 0.45$, while for $d_1 = 0.75$ the values of Ψ decrease linearly to zero.

In order to find a formula for η_c, we look again at equation (8) and write it as $s = (2\eta - 1)/2^k \left[2^k - \sum_{x=k/2+1}^{k+1} \binom{k+1}{x}(1+s)^x(1-s)^{k+1-x}\right]$. Observe that the term $2^k - \sum_{x=k/2+1}^{k+1} \binom{k+1}{x}(1+s)^x(1-s)^{k+1-x}$ contains only odd powers of s, and that s is a factor of the expression. Neglecting the terms of order s^4 and higher we obtain $2^k - \sum_{x=k/2+1}^{k+1} \binom{k+1}{x}(1+s)^x(1-s)^{k+1-x} = s(a_0 + a_2 s^2)$, where $a_0 < 0$ and $a_2 > 0$ are real coefficients. Thus, ignoring the solution $s = 0$, we can solve for η to get

$$\eta - \eta_c = \frac{2^{k-1}a_2}{-a_0^2}s^2 \qquad \text{where} \qquad \eta_c = \frac{1}{2} + \frac{2^{k-1}}{a_0}. \tag{11}$$

One can check that (11) yields the critical values η_c mentioned above for $k = 2$ and $k = 4$. Since $a_2 > 0$ formula (11) yields real solutions for $\eta < \eta_c$, so a phase transition occurs at $\eta = \eta_c$. Thus the values of the order parameter ψ near the transition can be obtained as follows in this case:

$$\psi = \begin{cases} \frac{-a_0\sqrt{\eta_c - \eta}}{\sqrt{2^{k-1}a_2}} & \text{for} \quad \eta < \eta_c \\ 0 \quad \text{for} \quad \eta > \eta_c \end{cases}$$

On the other hand, if the parameter d_1 does not satisfy $\frac{k}{2(k+1)} < d_1 \leq \frac{k+2}{2(k+1)}$ when $d_2 = 1$, then the sum $\sum_x \binom{k+1}{x} \neq 2^k$, $x \in [d_1(k+1), d_2(k+1)] \cap \mathbf{N}$, and thus $s = 0$ is not a fixed point. In this case there is no dynamical phase transition. Moreover, a large k makes the interval $\left(\frac{k}{2(k+1)}, \frac{k+2}{2(k+1)}\right]$ very narrow, so most of the values of d_1 will not yield a dynamical phase transition. The same is true for odd values of k, matching the numerous simulation results. More generally, observe that $s = 0$ is a solution of (8) if and only if the parameters d_1, d_2, and k are such that $\sum_x \binom{k+1}{x} = 2^k$, $x \in [d_1(k+1), d_2(k+1)] \cap \mathbf{N}$. Any such sum would have to span the middle terms of the binomial expansion of 2^{k+1}, since otherwise the sum will be smaller than 2^k. Thus, for k even this means

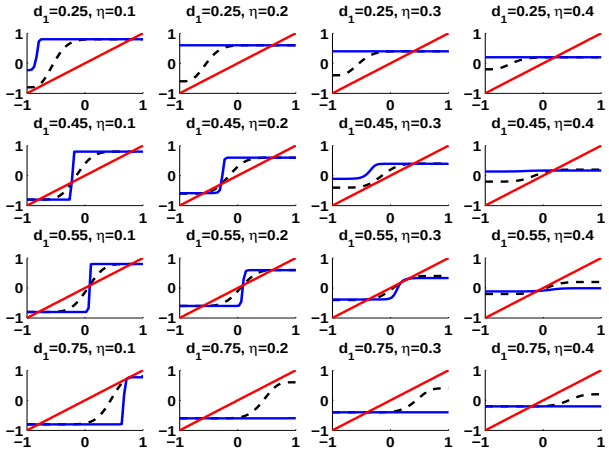

FIGURE 7. The graphs of $g(s)$ (interrupted line) and $g^4(s)$ (continuous line) versus s for the function $g(s) = (2\eta - 1)\left[1 - \frac{1}{2^k}\sum_x \binom{k+1}{x}(1+s)^x(1-s)^{k+1-x}\right]$ given by equation (8), plotted on $[-1,1] \times [-1,1]$ together with the first diagonal. Here $k = 6, d_2 = 1$ and the values of d_1 and η are specified in the subplots. Small values of η generate multiple fixed points closer to ± 1, while large η generate fixed points close to the origin. Higher order iterates do not induce more complexity.

at least $\binom{k+1}{k/2} + \binom{k+1}{k/2+1} = 2\binom{k+1}{k/2}$. By a simple computation one can show that $2\binom{k+1}{k/2} > 2^k$. For k odd the sum spans at least $\binom{k+1}{(k-1)/2} + \binom{k+1}{(k-1)/2+1} = \binom{k+2}{(k-1)/2+1} > 2^k$ by a similar computation. Thus, the origin is a fixed point of (8) only when k is even, $d_2 = 1$, and $d_1 \in \left(\frac{k}{2(k+1)}, \frac{k+2}{2(k+1)}\right]$, or when $d_1 = 0$, and $d_2 \in \left[\frac{k}{2(k+1)}, \frac{k+2}{2(k+1)}\right)$. Otherwise there cannot be a dynamical phase transition such that $\psi = 0$ for values of the noise parameter η greater than a critical value. However, the values of ψ approach zero as η approaches $1/2$.

We note here that a similar behavior is observed for varying number of parents. Define $s_j(t) = \frac{1}{M_j}\sum_{c_n \in \hat{k}_j}(2c_n(t) - 1)$ and $\phi_j(t) = \frac{1}{M_j}\sum_{c_n \in \hat{k}_j} c_n(t)$, where M_j is the number of nodes with k_j parents, $j = 1, 2, \ldots, J$ and $\hat{k_j}$ is the collection of nodes with k_j parents. Observe that $\sum_{j=1}^{J} M_j = N$ and $\cup_{j=1}^{J}\hat{k_j} = \{c_1, c_2, \ldots, c_N\}$. Consider $g_j(c_{n_1}, c_{n_2}, \ldots, c_{n_{k_j+1}}) = \chi_{[d_1^j(k_j+1), d_2^j(k_j+1)]}\left(\sum_{l=1}^{k_j+1} c_{n_l}\right)$ and $c_n(t+1) = g_j(c_{n_1}, c_{n_2}, \ldots, c_{n_{k_j+1}})$ with probability $1-\eta_j$, and $c_n(t+1) = 1-g_j(c_{n_1}, c_{n_2}, \ldots, c_{n_{k_j+1}})$ with probability η_j for nodes c_n in class $\hat{k_j}$. We obtain $I_j(t) = \sum_x \binom{k_j+1}{x}\phi_j(t)^x(1-\phi_j(t))^{k_j+1-x}$, where $x \in [d_1^j(k+1), d_2^j(k+1)] \cap \mathbf{N}$, and $\phi_j(t+1) = I_j(t)(1-\eta_j) + (1-I_j(t))\eta_j$. Then $\phi(t) = \sum_{j=1}^{J}\frac{M_j}{N}\phi_j(t)$ and one needs to find the fixed points of the individual s_j's to obtain $\Psi = \sum_{j=1}^{J}\frac{M_j}{N}|s_j|$.

To identify the behavior for the case of varying number of parents, the authors have performed simulations with two possible values of k, and the plots suggest again a decreasing trend of Ψ as the corresponding noise parameters η_1 and η_2 are increased. However, the values of Ψ do not necessarily converge to zero, due to the combined effect of the two different rules and parameter sets. For smaller η values Ψ tends to be closer to 1, while for large η values Ψ tends to be closer to 0. For combinations involving even connectivity values, we can again observe a dynamical phase transition at certain critical values of the η parameters. For most combinations though, there are no critical values of the noise parameters that indicate a dynamical phase transition.

7. Conclusions

In conclusion, this paper presents an in-depth study of a single generalized cellular automaton rule on Boolean networks with fixed or varying connectivity. We consider a Boolean network governed by a generalization of ECA Rule 22 that can be regarded as a Boolean linear threshold function typical for neural networks, or as a biologically meaningful Boolean function with activating or inhibiting inputs. By varying the parameters of the Boolean rule one can consider biases towards the activators or the inhibitors of a given node. We analyze the network dynamics by comparing simulated dynamics with the analytical description. In general we observe that large connectivity generates stability at the origin, so the nodes are inactivated eventually, while smaller connectivity can induce either order, with bifurcations and multiple attractors, or chaos. Moreover, the reaction of the system to stochastic noise is investigated. We show that for some parameter combinations there are critical values of the noise parameters indicating a dynamical phase transition. More precisely, when the noise parameter surpasses certain critical values the nodes are activated or inactivated in a random manner. For smaller values of the noise parameter, more nodes tend to be in the same state, that is either active or inactive. However, in the context of the network considered in this paper there are parameter combinations for which such a transition may not occur, so there is a certain bias towards either the active or the inactive nodes for all noise parameter values.

A natural continuation of this research would be analyzing asynchronous updates useful in the analysis of systems composed of multiple interacting components. Similar work has been performed for example in ([7], [21], [28]) for other types of Boolean networks. Allowing multiple Boolean rules would be of interest as well. Probabilistic Boolean networks in which a node can be updated according to more than one Boolean rule to account for natural variations and disturbances in the system have been studied for example in [2]. Such an approach would provide a much more realistic model for biological cellular networks whose update schemes are dependent upon various protein interactions ([5], [6]). One could consider a similar noise procedure in the context of probabilistic Boolean networks, and generalize to a wider variety of Boolean rules. Involving techniques such as Fourier transforms, one could study the existence of critical noise values corresponding to dynamical phase transitions.

On the other hand it would be of interest to see a comparison of these results with other methods for state-space descriptions focusing on sizes of the attractors and their basins of attraction like the basin entropy ([29], [30]), as a measure of the complexity of information that such a network or ensembles of such networks are capable of storing.

Another interesting topic would be introducing other types of noise in the system to determine the stability of the system to perturbations ([20], [31]). For instance the work in [20] has shown that noise induction into a system governed by the ECA Rule 126 has a stabilizing effect on the dynamics of the system. On the other hand it would be of interest to tackle the topic of information propagation in such Boolean networks subject to noise. This kind of work has been recently developed in the context of perturbation avalanches in Boolean networks by Rämö et.al. [32].

The topic of synchronization of Boolean networks is also of interest especially in areas such as neural networks ([23], [24], [33], [34]). An analysis of deterministic or stochastic synchronization of networks governed by the generalized ECA Rule 22 of this paper could yield interesting results.

Taking into account the topology of the network as opposed to randomly selecting the parent nodes is another avenue of study. As observed in ([11], [12]), the variation of topology of the network from a random to regular or scale-free network has a clear impact on pattern formation. Embedding the topology in the network model could lead to interesting results regarding the effect of topology on the dynamics of the system.

References

[1] Wuensche A., *Basins of Attraction in Network Dynamics: A Conceptual Framework for Biomolecular Networks*, In Schlosser G., Wagner G.P. (eds), Chicago University Press, Chicago, 2004, pp. 288-314.

[2] Shmulevich I., Dougherty E.R., Zhang W., *From Boolean to Probabilistic Boolean Networks as Models for Genetic Regulatory Networks*, Proceedings of the IEEE, Vol. 90, 11 (2002), p. 1778-1792.

[3] Brun M., Dougherty E. R., Shmulevich I., *Steady-State Probabilities for Attractors in Probabilistic Boolean Networks*, Signal Processing, Vol. 85, No. 4, pp. 1993-2013, 2005.

[4] Lähdesmäki H., Hautaniemi S., Shmulevich I., Yli-Harja O., *Relationships Between Probabilistic Boolean Networks and Dynamic Bayesian Networks as Models of Gene Regulatory Networks*, Signal Processing, Vol. 86, No. 4, pp. 814-834, 2006.

[5] Heidel J., Maloney J., Farrow C., Rogers J.A., *Finding Cycles in Syncrhonous Boolean Networks with Applications to Biochemical Systems*, Intl. J. Bifurcation Chaos Appl. Sci. Eng. 13 (2003) 535-552.

[6] Klemm K., Bornholdt S., *Topology of Biological Networks and Reliability of Information Processing*, PNAS, 102 (2005), p. 18414-18419.

[7] Klemm K., Bornholdt S., *Stable and unstable attractors in Boolean networks*, Phys. Rev. E 72, 055101 (2005).

[8] Raeymaekers L., *Dynamics of Boolean networks controlled by biologically meaningful functions*, Journal of Theoretical Biology, 218, p. 331-341, 2002.

[9] Aldana M., Cluzel P., *A Natural Class of Robust Networks*, PNAS 100 (2003), p. 8710-8714.

[10] Huepe C., Aldana-González M., *Dynamical Phase Transition in a Neural Network Model with Noise: An Exact Solution*, Journal of Statistical Physics, 108, Nos. 3/4, 2002.

[11] Marr C., Hütt M-T., *Topology Regulates Pattern Formation Capacity of Binary Cellular Automata on Graphs*, Physica A, 354 (2005), p. 641662.

[12] Marr C., Hütt M-T., *Similar Impact of Topological and Dynamic Noise on Complex Patterns*, Physics Letters A, 349 (2006) 302-305.

[13] Wolfram S., *A New Kind of Science*, Wolfram Media, Champaign, 2002.

[14] Kauffman S.A., *Self-Organization and Adaptation in Complex Systems*, In: *The Origins of Order: Self-Organization and Selection in Evolution*, Oxford University Press, New York (1993), p. 173-235.

[15] Wolfram S., *Cellular Automata as Models of Complexity*, Nature 311, 419 (1984).

[16] Chua L.O., Yoon S., Dogaru R., *A nonlinear dynamics perspective of Wolframs new kind of science. Part I: Threshold of Complexity*, International Journal of Bifurcation and Chaos, Vol. 12, 12 (2002), p. 2655-2766.

[17] Matache M.T., Heidel J., *Random Boolean Network Model Exhibiting Deterministic Chaos*, Phys. Rev. E 69, 056214, 2004, 10 pages.

[18] Matache M.T., Heidel J., *Asynchronous Random Boolean Network Model Based on Elementary Cellular Automata Rule 126*, Phys. Rev. E 71, 026232 (2005), 13 pages.

[19] Deng X., Geng H., Matache M.T., *Dynamics of Asynchronous Random Boolean Networks with Asynchrony Generated by Stochastic Processes*, BioSystems 88 (2007), p. 1634.

[20] Goodrich C.S., Matache M.T., *The Stabilizing Effect of Noise on the Dynamics of a Boolean Network*, Physica A 379 (2007) 334-356.

[21] Matache M.T., *Asynchronous Random Boolean Network Model with Variable Number of Parents based on Elementary Cellular Automata Rule 126*, IJMPB 20 (2006) p. 897-923.

[22] Goodman R., Matache M.T., *Dynamics of Directed Boolean Networks under Generalized Elementary Cellular Automata Rules, with Power-Law Distributions and Popularity Assignment of Parent Nodes*, to appear in Complex Systems 17(4) (2008).

[23] Andrecut M., *Mean Field Dynamics of Random Boolean Networks*, J. Stat. Mech., P02003 (2005).

[24] Hung Y-C., Ho M-C., Lih J-S., Jiang I-M., *Chaos Synchronization of Two Stochastically Coupled Random Boolean Networks*, Physics Letters A, 356, 2006, p. 35-43.

[25] Hu S.-T., *Threshold logic*, University of California Press, Berkeley, 1965.

[26] Anthony M., *Accuracy of Classification by Iterative Linear Thresholding*, Proceedings of the Workshop on Discrete Mathematics and Data Mining, 3rd SIAM International Conference on Data Mining, San Francisco, May 2003.

[27] Alligood K.T., Sauer T.D., Yorke J.A., *Chaos: An Introduction to Dynamical Systems*, Springer-Verlag (1996).

[28] Rohlfshagen P., DiPaolo E.A., *The Circular Topology of Rhythm in Asynchronous Random Boolean Networks*, Biosystems 73 (2004), p. 141-152.

[29] Krawitz P., Shmulevich I., *Basin entropy in Boolean network ensembles*, Physical Review Letters 98, 158701, 2007.

[30] Krawitz P., Shmulevich I., *Basin entropy in Boolean network ensembles*, Physical Review E 76, 036115, 2007.

[31] Chaves M., Albert R., Sontag E.D., *Robustness and fragility of Boolean models for genetic regulatory networks*, J. Theoretical Biology 235, p. 431-449, 2005.

[32] Rämö P., Kauffman S., Kesseli J., Yli-Harja O., *Measures for information propagation in Boolean networks*, Physica D: Nonlinear Phenomena, Vol. 227, Issue 1, 1 March 2007, p. 100-104.

[33] Morelli L.G., Zanette D.H., *Synchronization of stochastically coupled cellular automata*, Phys. Rev. E 58 (1), 1998, R8.

[34] Fan J., Li X., Wang X.F., *On synchronous preference of complex dynamical networks*, Physica A, 355, p. 657-666, 2005.